Performance and robustness analysis in adaptive and non-adaptive GMVC applied to a MISO process

Nelson N. N. Yamaguti * **Daniel A. M. da Silva** * **Bruno G. Dutra** * **Antonio S. Silveira** *

* *Institute of Technology, Federal University of Pará, Belém, 66075-110, Brazil (e-mail: nelson.yamaguti@itec.ufpa.br, daniel.abreu@itec.ufpa.br, brunodutra@ufpa.br, asilveira@ufpa.br).*

Abstract: This paper proposes the performance and robustness analysis of the positional and incremental *Generalized Minimum Variance Control* (GMVC), designed in adaptive and non-adaptive topology, experimentally in a Multiple-Input and Single-Output (MISO) physical process, which has aerodynamics similar to several aerospace processes, where performance and robustness indexes are evaluated, widely studied in academia and industry. In addition to evaluating the design of the didactic plant to prove the efficiency of control techniques with the use of a complementary filter together with the responses of the sensors. The model is identified with the least squares estimation algorithms, being applied recursively to the adaptive algorithms. The results shows that GMVC with incremental action in the ARIX model in the self-tuning topology proved to be more efficient.

Keywords: Generalized Minimum Variance Control; Least Squares Estimation; MISO process; Performance; Robustness; Self-Tuning Control.

1. INTRODUCTION

Several processes require controllers to obtain reference tracking and rejection of unwanted disturbances (Åström and Wittenmark, 2013b). Currently, with the spread of predictive control, it has been widely addressed and applied in the study of process control, because its characteristics, such as robustness, guarantee of reference tracking, disturbance rejection and prediction of the output, those are advantages that make these controllers very useful and necessary for the advancement of studies in the field of control theory. Among these controllers, there is the Generalized Minimum Variance Controller (GMVC), which is a Model Based Predictive Controller (MBPC) that has been used successfully in process control area and has been gaining space in industry.

The algorithms based in MBPC uses the models of the system to be controlled along with certain parameters that aim to minimize a cost function, to design a control law that is applied to the system (Fernandez-Camacho and Bordons-Alba, 1995). However, when the model is unknown, designers must resort to adaptive control techniques, that is, when the formulation of the control law, which requires the model, is updated at each iteration, since the model is identified at each sampling time (Åström and Wittenmark, 2013a). In the proposed work, we used the technique of identification parametric using the Recursive Least Squares algorithm, which has been widely used in academia and industry for process modeling (Aguirre, 2004; Coelho and dos Santos Coelho, 2004; Da Silva et al., 2021a).

The importance of evaluating the performance and robustness of predictive controllers, whether adaptive or not, is to obtain measures that qualify and quantify such controllers for academic or industrial applications. According to De Barros Araújo et al. (2016), for complex processes, MBPCs have been widely used and indexes, as Phase Margin (PM), Gain Margin (GM), among others are analysed. Therefore, the use of a plant or a prototype to test the effectiveness of the identification and control is important and very motivating, since, in this way, the control algorithm developer can analyse an application in a real system. In the present work, we used a MISO system to evaluate the efficiency of controllers implemented in a highly complex process, in addition to evaluating the use of the complementary filter and the sensors instrumentation used to acquire the reading of sensor data.

According to the controller design, the performance indexes can change for better or worse, for this reason, the proposed work aims to analyze the performance of the adaptive and non-adaptive topology GMVC in a MISO system in terms of reference tracking, disturbances rejection, prediction of the outputs and robustness of the controller. This work is organized as follows. The second section presents the process composition. The third section, the importance and appliance of sensors and filters used are presented to explain the signal reading. The model and the estimation are presented in the fourth section. The GMVC in positional and incremental topology are presented in the fifth section. The robustness and performance indexes used are presented in the sixth section. The results are analyzed in the seventh section and the conclusions of the research will be made in the eighth section.

2. PROCESS COMPOSITION

The didactic process used in this research, is the same developed by Yamaguti et al. (2021), this didactic process has dynamics similar to heavy delivery vehicles in the military aerospace sector, such as the Boeing CH-47 Chinook, where propulsion is carried out by two propellers and the control variable is the angular position of the moving component of the system, therefore it is a MISO system with two inputs and one output.

The prototype was developed using the Computer Aided Design application (CAD) 3D Inventor®. The design created with the Inventor® software is shown in Figure 1.a. Then, the project which was manufactured on a 3D printer, is shown in Figure 1.b, where can be seen various components to the operation of the didactic process.

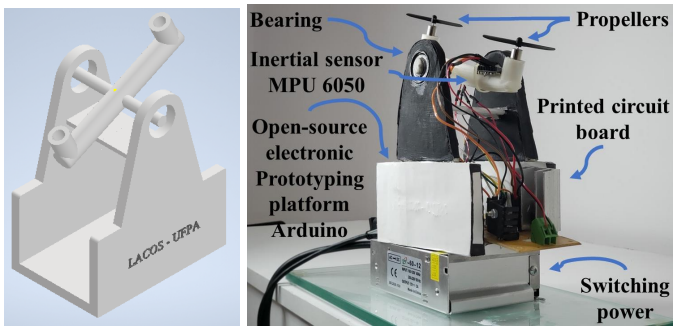

a. 3D model. b. Process developed for the research

Figure 1. Didactic plant

The electrical circuit diagram was created using ISIS-Proteus® software, the Figure 2 shows this diagram planned to read the signal from the MPU-6050, used as the angular sensor, and for sending the signal from the control action (signal generated by an Arduino UNO output, which is an open source electronic prototyping platform based on the ATmega328P microcontroller), and power from an external source.

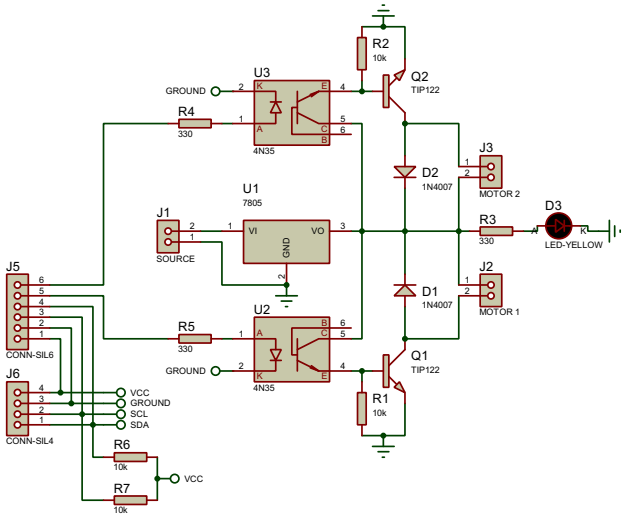

Figure 2. Schematic of motors drive circuit, developed in ISIS-Proteus® software.

3. SIGNAL READING

The sensor used to read the angular position of the didactic process was the inertial sensor (IMU – Inertial Measurement Units) MPU-6050, which makes use of a microelectromechanical system (MEMS – Microelectromechanical Systems) which enables the MPU-6050 module to contain gyro and accelerometer sensors.

3.1 Gyrometer

For Bueno and Romano (2014) and Santos et al. (2017), the gyrometer reads values referring to the angular velocity, in this way, to obtain values referring to the angular position, knowing the conditions, the initial signal must be integrated into the time. Thus, the Difference Equation (DE) that performs the integration operation is given by:

$$x(k) = x(k-1) + \omega(k)T_s \tag{1}$$

where, x, k, ω and T_s represent the estimated angular position, the instant of time, the angular velocity read measurements and the sampling period, respectively.

This integration will result in a considerable rise in error, which will increase with each output signal iteration. This cumulative error is known as a drift error. A possible solution to this problem is using the following High Pass Filter (HPF) on the output signal:

$$\theta_{gyro}(k) = \beta\theta_{gyro}(k-1) + x(k) - x(k-1) \tag{2}$$

$$\beta = e^{-\frac{T_s}{\tau}} \tag{3}$$

where θ_{gyro} is the filtered angular position and β is the time constant that regulates the low cutoff frequency of the HPF through the relation (3) and in (3), τ is the time constant. Observing (1) and (2), it can be concluded that the output of the integrator and the input of the HPF are connected in cascade. So, substituting (1) into (2):

$$\theta_{gyro}(k) = \beta\theta_{gyro}(k-1) + \omega(k)T_s \tag{4}$$

3.2 Accelerometer

Taking into consideration three-dimensional space, the orientation of the acceleration can be calculated by

$$\theta(k) = tg^{-1}\left[\frac{a_y(k)}{\sqrt{a_x^2(k) + a_z^2(k)}}\right].\frac{180}{\pi} \tag{5}$$

where θ, a_y, a_x and a_z correspond to the resulting orientation, to the accelerations in y, x and z, respectively. According to Barrera Prieto (2018), accelerometers reads a lot of high-frequency noise, a possible way to attenuate these noises is with the implementation of following Low Pass Filter (LPF):

$$\theta_{acel}(k) = \beta\theta_{acel}(k-1) + (1-\beta)\theta(k-1) \tag{6}$$

where θ_{acel} is the filtered acceleration orientation and θ is the unfiltered acceleration orientation, both in the discrete time domain.

3.3 Complementary filter

According to Barrera Prieto (2018), the gyroscope is responsible for accurately measuring high-frequency behaviors and the accelerometer, with its zero stationary error measurement, is responsible for measuring low-frequency behaviors. In this way, the Complementary Filter (CF) is used to take advantage of each sensor in order to obtain a more reliable reading. The CF can be calculated using the following equation

$$\theta_x(k) = \alpha\left[\theta_x(k-1) + \theta_{gyro}(k)T_s\right] + (\alpha - 1)\,\theta_{acel}(k) \quad (7)$$

where θ_x is the CF output (estimated angular position) and α is the fusion complementation coefficient, its value is selected based on experimental tests. For this work, the value of $\alpha = 0.98$ was selected.

4. ESTIMATION OF DAMPED PENDULUM MODEL

For practical purposes, the system identification method used, was the application of Least Squares (LS). To control the MISO process, such as the process used in this paper, the controllers were designed using a strategy to act in a decentralized manner (Yamaguti et al., 2021; Coelho and dos Santos Coelho, 2004).

The Figure 3 shows the MISO system block diagram, considering the Auto Regressive with inputs eXogenous (ARX) model, as the process has two inputs ($u_1(k)$ and $u_2(k)$: two propulsion engines) and one output ($y(k)$: angular position of the didactic process), it is possible to write the output signal as (8).

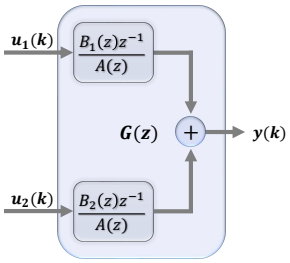

Figure 3. MISO system block diagram within ARX model.

$$y(k) = \frac{B_1(z)z^{-1}}{A(z)}u_1(k) + \frac{B_2(z)z^{-1}}{A(z)}u_2(k) \quad (8)$$

where $B_1(z)$ and $B_2(z)$ are the polynomials filtering the input $u_1(k)$ and $u_2(k)$, respectively.

Due the system has an underdamped dynamic, considering that the estimated discrete model is second order, (8) can be represented as a difference equation, as in (9).

$$\begin{aligned} y(k) = & -a_1 y(k-1) - a_2 y(k-2) \\ & + b_{10}u_1(k-1) + b_{11}u_1(k-2) \\ & + b_{20}u_2(k-1) + b_{21}u_2(k-2) \end{aligned} \quad (9)$$

4.1 Non-Recursive Least Squares

According to Yamaguti et al. (2021) Non-Recursive Least Squares (NRLS) estimator is designed taking into account two factors: knowledge of the dynamics of the process, and according to the value of the squared Pearson correlation coefficient (R^2):

$$R^2 = 1 - \frac{\sum_{k=1}^{N}\left[y(k) - \hat{y}(k)\right]^2}{\sum_{k=1}^{N}\left[y(k) - \bar{y}\right]^2} \quad (10)$$

where $\hat{y}(k)$, $\bar{y}$ and N correspond to estimated output, average output and number of samples, respectively. According to Coelho and dos Santos Coelho (2004), for many practical applications, values of R^2 between 0.8 and 1.0 can be considered sufficient. After identification via NRLS, a value of $R^2 = 0.972$ was obtained.

Thus, using (9), the vector containing the read data (measures vector – $\boldsymbol{y}$), presented in (11), the matrix encompassing inputs and output data of the system (matrix of regressors – Φ), presented in (12), and the vector of estimated parameters (θ), presented in (13), may be determined.

$$\boldsymbol{y^T} = [y(1)\ y(2)\ \ldots\ y(N)] \quad (11)$$

$$\Phi = \begin{bmatrix} -y(1) & 0 & u_1(1) \\ -y(2) & -y(1) & u_1(2) \\ \vdots & \vdots & \vdots \\ -y(N-1) & -y(N-2) & u_1(N-1) \\ 0 & u_2(1) & 0 \\ u_1(1) & u_2(2) & u_2(1) \\ \vdots & \vdots & \vdots \\ u_1(N-2) & u_2(N-1) & u_2(N-2) \end{bmatrix} \quad (12)$$

$$\theta^T = [a_1\ a_2\ b_{10}\ b_{11}\ b_{20}\ b_{21}] \quad (13)$$

After defining (11), (12) and (13), the following algebraic equation appears:

$$\boldsymbol{y} = \Phi\theta \quad (14)$$

According to Coelho and dos Santos Coelho (2004); Yamaguti et al. (2021), to calculate θ using (14), it will be necessary that Φ is a square matrix, however Φ is a matrix of order $\Phi_{N,6}$. Thus, according to Aguirre (2004), it is necessary to apply the pseudo-inverse matrix. As a result, the solution of non-recursive least squares estimator was determined by computing θ as (15).

$$\theta = [\Phi^T\Phi]^{-1}\Phi^T\boldsymbol{y} \quad (15)$$

Using a sequence of steps with amplitude of $1.5V$, $3V$ and $2V$, being applied to u_1 at $0s$, $7s$ and $9s$, respectively, with sampling period $T_s = 0.0135s$; and a sequence of steps with amplitude of $2V$, $0V$ and $1V$, in the same instants mentioned before, it was possible to obtain the output data and estimate the following parameters vector:

$$\theta^T = [-1.111\ 0.184\ 0.246\ -1.117\ 0.952\ -0.404] \quad (16)$$

4.2 Recursive Least Squares

In the Recursive Least Squares (RLS) method, the model to be identified, as it uses real-time measurements, it must be iterative; therefore, the model parameters are updated at each sampling period (Da Silva et al., 2021a).

Before starting the iterative calculations, the covariance matrix P was initialized as a diagonal matrix of order 6, because there are six parameters to be estimated, where the elements of the main diagonal are equal to 100 to give the algorithm a good convergence capability of the estimated parameters and θ was initialized with the same values in (16).

Then entering the iterative part, Φ, presented in (12), is now calculated in each iteration as follow:

$$\begin{aligned}\Phi^T = [\, &-y(k-1)\ -y(k-2)\ u_1(k-1) \\ &u_1(k-2)\ u_2(k-1)\ u_2(k-2)\,]\end{aligned} \tag{17}$$

then the estimation gain (L) is calculated by:

$$L = \frac{P\Phi}{\lambda + \Phi^T P \Phi} \tag{18}$$

where according to Coelho and dos Santos Coelho (2004), the forgetting factor (λ), provides the RLS algorithm the adaptability in estimating parameters in time-varying or non-linear processes. In order to weigh the parameters estimated essentially on the last data samples, $\lambda = 0.98$ was used.

Then the estimated output, y_{est}, is calculated by (19), then the estimated error, e_{est}, is calculated by (20), and finally, the estimated parameters, θ, are updated by (21):

$$y_{est} = \Phi^T \theta \tag{19}$$

$$e_{est} = y(k) - y_{est} \tag{20}$$

$$\theta = \theta + L e_{est} \tag{21}$$

Due the GMVC design is model-based, in self-tuning control, as the identification parameters are updated with each iteration, the tuning parameters of the law control of GMVC are also updated with each iteration.

5. GENERALIZED MINIMUM VARIANCE CONTROL

5.1 Positional

For this MISO system described by an ARX model, the GMVC goal is to determine the control signals $u_1(k)$ and $u_2(k)$ that minimizes the cost function $J = E[\phi(k+d)]$, where $E[.]$ indicates the expected value (or mathematical expectation) and the generalized output is

$$\begin{aligned}\phi(k+d) = \ &P(z)y(k+d) - T(z)y_r(k+d) \\ &+Q_1(z)u_1(k) + Q_2(z)u_2(k)\end{aligned} \tag{22}$$

where d is the prediction horizon and the polynomials $P(z)$, $T(z)$, $Q_1(z)$ and $Q_2(z)$ weighting the behavior of output, reference and inputs signals, respectively. To facilitate the project, it was made $P(z) = T(z) = 1$. According to Silveira et al. (2012), the generalized output in (22), $y(k+d)$ is a future measurement not available at instant k, thus it must be predicted in order to work with $\phi(k+d)$. To achieve the prediction, the Diophantine equation in (23) provides two auxiliary polynomial relations:

$$1 = A(z)E(z) + F(z)z^{-1} \tag{23}$$

therefore, solving the Diophantine equation, the design of the GMV is summarized in determining the polynomials $E(z)$ and $F(z)$. The order of polynomial $E(z)$ is determined by $n_e = d - 1$ and the order of polynomial $F(z)$ is determined by $n_f = n_a - 1$, so for the case of one step ahead prediction ($d = 1$) and knowing that the system is of second order ($n_a = 2$):

$$E(z) = 1 \quad \text{and} \quad F(z) = f_0 + f_1 z^{-1} \tag{24}$$

so, solving (23), it is concluded that:

$$f_0 = -a_1 \quad \text{and} \quad f_1 = -a_2 \tag{25}$$

To finalize the project, the polynomials $Q_1(z)$ and $Q_2(z)$ are defined as:

$$Q_1(z) = q_1\Delta \quad \text{and} \quad Q_2(z) = q_2\Delta \tag{26}$$

where q_1 and q_2 tune the control efforts for each input, and the $\Delta = 1 - z^{-1}$ is the incremental action to guarantee null error in steady state. Thus, looking at Figure 4, the control laws are given by:

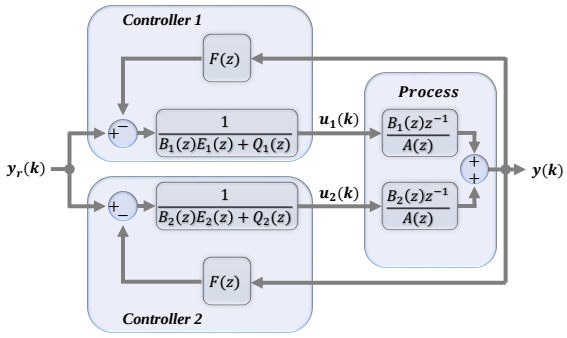

Figure 4. Block diagram of GMV in MISO system.

$$\begin{aligned}u_1(k) = \frac{1}{b_{10}+q_1}\ &[y_r(k+1) - f_0 y(k) - f_1 y(k-1) \\ &-(b_{11}-q_1)u_1(k-1)] \\ u_2(k) = \frac{1}{b_{20}+q_2}\ &[y_r(k+1) - f_0 y(k) - f_1 y(k-1) \\ &-(b_{21}-q_2)u_2(k-1)]\end{aligned} \tag{27}$$

5.2 Incremental

This time, in the case of the incremental GMVC project, the Auto-Regressive Integrated with eXogenous Inputs (ARIX) model will be considered, in the same way, the

objective of the incremental GMVC will be to determine the control actions u_1 and u_2 that minimize the cost function $J = E[\phi(k+d)]$, where the generalized output will be expressed by

$$\begin{aligned}\phi(k+d) = \; & P(z)y(k+d) - T(z)y_r(k+d) \\ & +Q_1(z)\Delta u_1(k) + Q_2(z)\Delta u_2(k)\end{aligned} \tag{28}$$

the Diophantine equation for the ARIX model, is expressed by

$$1 = \Delta A(z)E(z) + F(z)z^{-1} \tag{29}$$

the polynomial $E(z)$ remains $E(z) = 1$, and the order of the polynomial $F(z)$ changes, because $n_f = n_{\Delta a} - 1$, therefore

$$E(z) = 1 \quad \text{and} \quad F(z) = f_0 + f_1 z^{-1} + f_2 z^{-2} \tag{30}$$

solving (29), it is concluded that:

$$f_0 = 1 - a_1; \quad f_1 = a_1 - a_2 \quad \text{and} \quad f_2 = a_2 \tag{31}$$

the control laws are given by:

$$\begin{aligned}\Delta u_1(k) = \; & \frac{1}{b_{10} + q_1}[y_r(k+1) \\ & -f_0 y(k) - f_1 y(k-1) \\ & -f_2 y(k-2) - b_{11}\Delta u_1(k-1)] \\ \Delta u_2(k) = \; & \frac{1}{b_{20} + q_2}[y_r(k+1) \\ & -f_0 y(k) - f_1 y(k-1) \\ & -f_2 y(k-2) - b_{21}\Delta u_2(k-1)]\end{aligned} \tag{32}$$

remembering that $\Delta u(k) = u(k) - u(k-1)$, so:

$$\begin{aligned}u_1(k) &= u_1(k-1) + \Delta u_1(k) \\ u_2(k) &= u_2(k-1) + \Delta u_2(k)\end{aligned} \tag{33}$$

6. PERFORMANCE AND ROBUSTNESS ANALYSIS

6.1 Performance analysis

The trade-off between performance and robustness is a key issue in control design (Åström and Wittenmark, 2013b). Therefore, the use of a quantitative measure that evaluates the implemented controller is interesting, since when these performance indicators are minimized, the control system is considered effective or performing within the desired standards, and these are chosen with an emphasis on the specifications considered important to the system (Araújo, 2017).

Integral Square Error (ISE) and Integral Squared control signal (ISU) are two examples of performance indexes that can measure the efficiency of a controller, those are used in discrete time domain (Araújo, 2017). ISE and ISU can be calculated with (34) and (35), respectively.

$$ISE = \frac{1}{N}\sum_{k=1}^{N}[e(k)]^2 \tag{34}$$

$$ISU = \frac{1}{N}\sum_{k=1}^{N}[u(k)]^2 \tag{35}$$

The stochastic and probabilistic evaluation of the signals can present other interesting variables in the evaluation of the performance of the systems to be controlled (Martins et al., 2019). In this way, evaluating the variance of the error (σ_e^2) and control (σ_u^2) signals is interesting to obtain a probabilistic and stochastic evaluation of the processing of digital signals. Those can be calculated, respectively, as (36) and (37)

$$\sigma_e^2 = \frac{1}{N}\sum_{k=1}^{N}[e(k) - \mu_e]^2 \tag{36}$$

$$\sigma_u^2 = \frac{1}{N}\sum_{k=1}^{N}[u(k) - \mu_u]^2 \tag{37}$$

where μ_e and μ_u are, respectively, the mean value of error and control signals.

6.2 Robustness analysis

Robustness indexes are required to qualify the implemented controller as "optimal". Among those indexes are Gain Margin (GM) and Phase Margin (PM), which are directly related to the robust stability of the process. The higher the values of these indexes, more robust (less sensitive to unwanted disturbances) the system is, on the other hand, the dynamic becomes slower (Araújo, 2017; Da Silva et al., 2021b).

According to Coelho et al. (2019), the GM is defined as the required variation in the open-loop gain, necessary to make the system unstable, and the PM also provides a measure of the relative stability, indicating how much transport delay can be included in the feedback loop before instability to occur.

Other two variables are interesting to achieve the values of GM and PM on the controlled system, the Sensitivity function (S_{sen}) and the Complementary Sensitivity (T_{com}), presented in (38) and (39), respectively.

$$S_{sen}(z) = \frac{1}{1 + G_c(z)G_p(z)} \tag{38}$$

$$T_{com}(z) = \frac{G_c(z)G_p(z)}{1 + G_c(z)G_p(z)} \tag{39}$$

where $G_c(z)$ and $G_p(z)$ are, respectively, the controller and the process discrete transfer functions.

The S_{sen} characterizes the effect of a external disturbance acting on the output of the control loop, therefore indicates how the closed-loop system is sensitivity to process changes, while T_{com} is the Closed Loop Transfer Function (CLTF) for set-point changes (Araújo, 2017; Seborg et al.,

2016; Skogestad and Postlethwaite, 2007; Silveira et al., 2012).

Through some equalities and mathematical movements, the CLTF ($T_{com}(z)$), of the process is obtained with the positional and incremental GMVC as, respectively, (40) and (41)

$$T_{com_{pos}}(z) = \frac{B(z)z^{-1}}{A(z)\left[B(z)+q_0\Delta\right]+B(z)F(z)z^{-1}} \quad (40)$$

$$T_{com_{inc}}(z) = \frac{B(z)z^{-1}}{B(z)\left[\Delta A(z)+F(z)z^{-1}\right]+\Delta A(z)q_0} \quad (41)$$

According to Skogestad and Postlethwaite (2007), the value of $S_{sen}(z)$ can be achieved as (42) for positional and incremental GMVC;

$$S_{sen}(z) = 1 - T_{com}(z) \quad (42)$$

The maximum values of the amplitude ratio of $S_{sen}(z)$ and $T_{com}(z)$ for all frequencies, respectively, M_S and M_T (known as resonant peak), provides useful robustness measures and also shows a control system design criterion. These functions can be described by (43) and (44).

$$M_S \triangleq max\left[S_{sen}(z)\right] \quad (43)$$

$$M_T \triangleq max\left[T_{com}(z)\right] \quad (44)$$

According to Skogestad and Postlethwaite (2007), with M_S and M_T is possible to achieve GM and PM, as (45) and (46), respectively. This mathematical relation is valid for all implemented controllers of the paper.

$$GM \geq max\left[\frac{M_S}{M_S-1}, \frac{M_T+1}{M_T}\right] \quad (45)$$

$$PM \geq max\left[2sin^{-1}\left(\frac{1}{2M_S}\right), 2sin^{-1}\left(\frac{1}{2M_T}\right)\right] \quad (46)$$

7. RESULTS

7.1 Non-adaptive GMVC tests

In all tests realized, the objective was to achieve the following closed-loop performance specifications: maximum overshoot less or equal than twenty percent ($M_p \leq 20\%$) and a stabilization period less or equal than one second ($t_s \leq 1s$). To achieve these specifications, for the non-adaptive case, the positional GMVC was tuned with $q_1 = -100$ and $q_2 = 100$, and incremental GMVC was tuned with $q_1 = -140$ and $q_2 = 140$. The Figures 5 and 6 show the curves obtained for the positional and incremental case, respectively:

The Figures 7.a and 7.b show the $S_{sen}(z)$ and $T_{com}(z)$ curves obtained from the responses to positional and incremental GMVC, respectively. In these figures it is possible to verify that at low frequencies, the singular

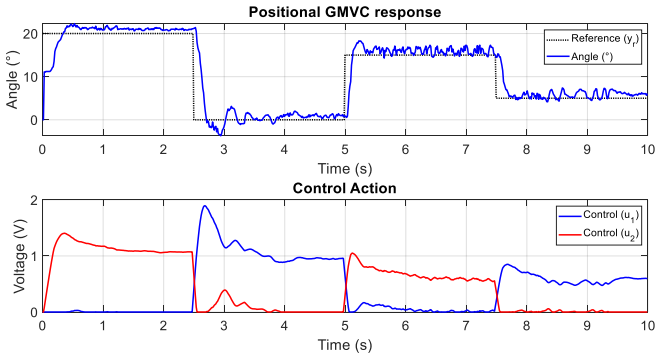

Figure 5. Upper graph: response (blue) and reference (black). Bottom graphic: controller 1 (blue) and controller 2 (red)

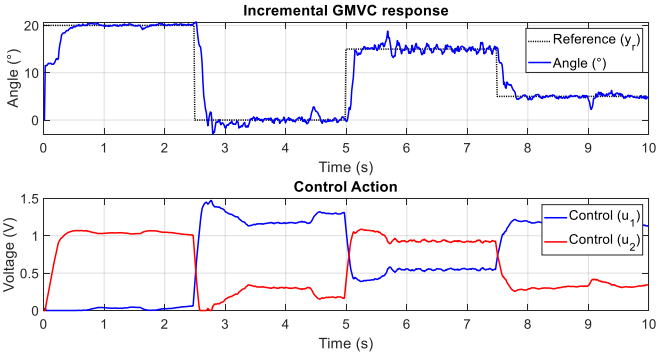

Figure 6. Upper graph: response (blue) and reference (black). Bottom graphic: controller 1 (blue) and controller 2 (red)

values of $T1(z)$ (referring to input u_1) and $T2(z)$ (referring to input u_2) on the logarithmic scale are null ($T1(z) = T2(z) \approx 0dB$), this means that the controllers achieve the good reference tracking with null offset error.

On the other hand, at high frequencies, the singular values of $T1(z)$ and $T2(z)$ become increasingly negative on the logarithmic scale ($T1(z) = T2(z) \to -50dB$), this ensures good capability of rejection of sensor noise.

Figures 7.a and 7.b show that at low frequencies, the singular values of $S1(z)$ and $S2(z)$ on the logarithmic scale are highly negative, which indicates that the system has good disturbance rejection. according to Seborg et al. (2016), it is desirable for the singular values of $S(z)$ to be null for all frequencies, but this is impossible.

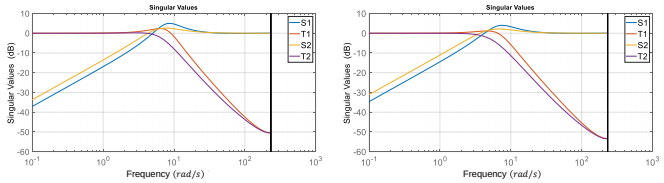

a. Positional GMVC Singular Values. b. Incremental GMVC Singular Values.

Figure 7. Singular Values

7.2 Self-Tuning GMVC tests

To achieve the same performance specifications in closed-loop ($M_p \leq 20\%$ and $t_s \leq 1s$), for the self-tuning case, the positional GMVC was tuned with $q_1 = -200$ and $q_2 = 200$, and incremental GMVC was tuned with $q_1 = -140$ and $q_2 = 140$. The Figures 8 and 9 show the curves obtained for the positional and incremental case, respectively:

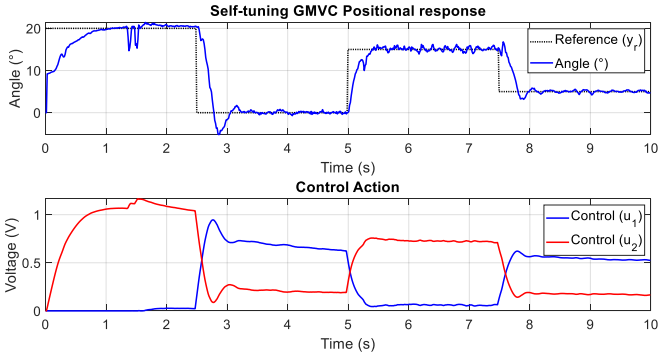

Figure 8. Upper graph: response (blue) and reference (black). Bottom graphic: controller 1 (blue) and controller 2 (red)

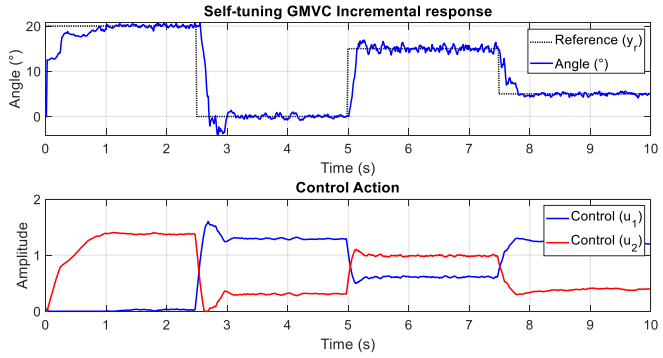

Figure 9. Upper graph: response (blue) and reference (black). Bottom graphic: controller 1 (blue) and controller 2 (red)

For the self-tuning cases, changes in GM and PM were verified during the iterations, the Figures 10.a and 10.b show the variation of the GM and PM for each process input in relation to time for the self-tuning positional case.

In Figure 10.a it is possible to observe that $GM1$ (referring to input u_1) remained most of the time around $8dB$ and while $GM2$ (referring to input u_2) around $32dB$. On the other hand, in Figure 10.b it is possible to observe that $PM1$ remained most of the time around 35° and while $PM2$ around 59°.

The Figures 10.c and 10.d represent the GM and PM histograms, respectively. The x-axis of Figure 10.c represents the GM and the x-axis of Figure 10.d represents the PM and the y-axis of Figures 10.c and 10.d represents the number of occurrences. thus, the histogram of Figure 10.c shows that the value of $GM1$ occurred more frequently around $8dB$ and $GM2$ around $32dB$, while the histogram of Figure 10.d shows that the value of $PM1$ occurred more frequently around 35° and $PM2$ around 59°.

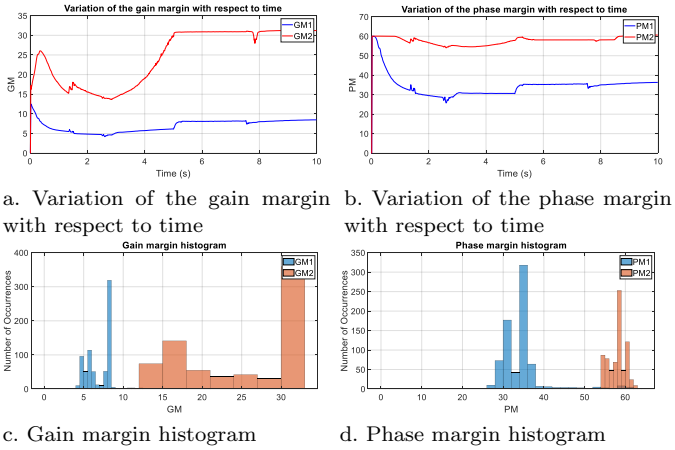

a. Variation of the gain margin with respect to time
b. Variation of the phase margin with respect to time
c. Gain margin histogram
d. Phase margin histogram

Figure 10. Analysis of the variation of gain and phase margins for the self-tuning positional case.

The statistical analysis of Figure 11 is similar to the analysis carried out in Figure 10, therefore, observing the Figures 11.a and 11.c, it is concluded that $GM1$ stayed most of the time around $21dB$ and $GM2$ around $49dB$ on the other hand, observing in Figure 11.b and 11.d, it is concluded that $PM1$ stayed most of the time around 53° and $PM2$ around 60°

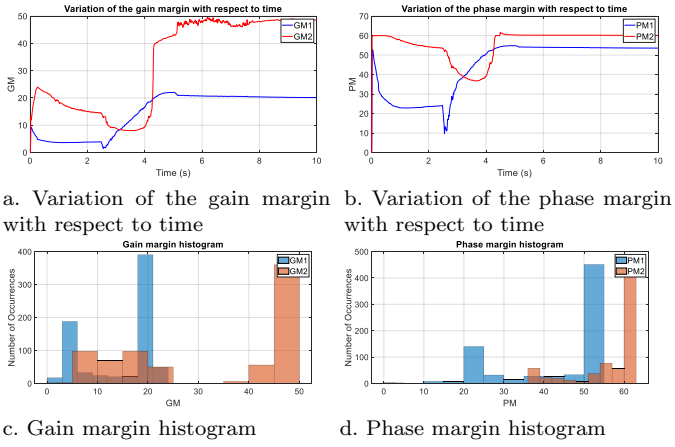

a. Variation of the gain margin with respect to time
b. Variation of the phase margin with respect to time
c. Gain margin histogram
d. Phase margin histogram

Figure 11. Analysis of the variation of gain and phase margins for the self-tuning incremental case.

Due to the variation of GM and PM during the iterations of the tests realized for the self-tuning case, ten Monte Carlo tests were performed to verify if these variations would follow some pattern, as shown in Figures 12 and 13, although the values of GM and PM vary with each test, it is possible to calculate expected values for each index.

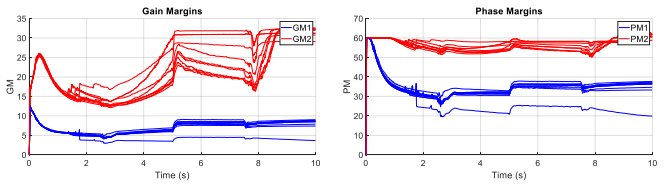

a. Gain Margin.
b. Phase margin.

Figure 12. Monte Carlo test for the positional self-tuning case

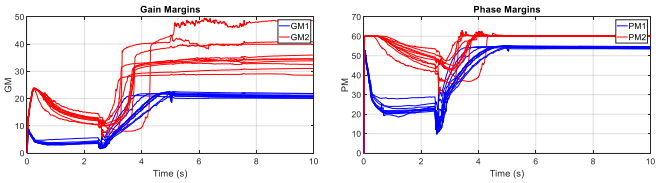

a. Gain Margin. b. Phase margin.

Figure 13. Monte Carlo test for the incremental self-tuning case

The indexes presented in Table 1 referring to the self-tuning case were calculated using an average of the ten Monte Carlo tests.

Table 1. Results of metrics used to evaluate the controllers

	Non-adaptive		Self-tuning	
	Positional	Incremental	Positional	Incremental
ISE	10.9912	10.0136	15.0815	9.5943
ISU	0.85241	1.2975	0.5812	1.4353
σ_e^2	10.3069	10.0097	15.0758	9.5837
σ_u^2	0.4459	0.38016	0.2180	0.4000
$GM1$	7.1729	8.6052	8.1944	21
$PM1$	44.7246	51.7512	34.3500	53.3500
$GM2$	11.6778	13.2028	21.4500	35.2
$PM2$	58.4396	60.0009	55.1000	60.35

8. CONCLUSIONS

Through the values presented in Table 1, it is noted that the ISE became smaller through the incremental action in the ARIX model in both topologies (self-tuning and non-adaptive), this means that in terms of reference tracking, the adaptive case proved to be more efficient. On the other hand, ISU was higher in the incremental control of both topologies (self-tuning and non-adaptive), so although the reference tracking is better for incremental cases, there was a higher energy consumption for this.

The results table also shows that the variance of the response and the control action is smaller in the incremental action in the ARIX model in the non-adaptive topology. However, in the self-tuning case, the incremental action resulted in a smaller response variance and a larger variance in the control action. Therefore, in terms of oscillation in the response, the incremental adaptive topology proved to be the best option.

The results table shows that the incremental action applied in the ARIX model for both topologies (self-tuning and non-adaptive) ensured higher values of $GM1$, $PM1$, $GM2$ and $PM2$. Therefore, it is noted that in terms of reference tracking, response oscillation and robustness, the GMVC with incremental action in the ARIX model in the self-tuning topology proved to be more efficient.

ACKNOWLEDGMENT

To the Federal University of Pará, to the Laboratory of Control and Systems (LACOS), to CNPQ and to CAPES.

REFERENCES

Aguirre, L.A. (2004). *Introdução à identificação de sistemas–Técnicas lineares e não-lineares aplicadas a sistemas reais*. Editora UFMG.

Araújo, R.d.B. (2017). Controladores preditivos filtrados utilizando otimização multiobjetivo para garantir offset-free e robustez. *Tese submetida ao Programa de Pós-Graduação em Engenharia de Automação e Sistemas. Universidade Federal de Santa Catarina.*

Åström, K.J. and Wittenmark, B. (2013a). *Adaptive control*. Courier Corporation.

Åström, K.J. and Wittenmark, B. (2013b). *Computer-controlled systems: theory and design*. Courier Corporation.

Barrera Prieto, F. (2018). Um estudo sobre arquiteturas de hardware para técnicas de fusão sensorial através do ekf e da estimação de estados baseada em filtros híbridos otimizados. *Dissertação submetida ao departamento de engenharia mecânica.Universidade de Brasília.*

Bueno, A.G. and Romano, R.A. (2014). Filtro complementar aplicado a medida de inclinação de plataformas móveis.

Coelho, A.A.R. and dos Santos Coelho, L. (2004). *Identificação de sistemas dinâmicos lineares*. Editora ufsc, Florianópolis: Ed. da UFSC.

Coelho, A.A.R., Jeronymo, D.C., and Araújo, R.d.B. (2019). *Sistemas dinâmicos: Controle clássico e preditivo discreto*. editora ufsc, Florianópolis: Ed. da UFSC.

Da Silva, D.A.M., da Silva, M.M., and de Barros Araújo, R. (2021a). Desenvolvimento de uma interface para identificação paramétrica de processos utilizando a estimação dos mínimos quadrados recursivos. In *2021 14th IEEE International Conference on Industry Applications (INDUSCON)*, 969–975. IEEE.

Da Silva, D.A.M., do Nascimento, A.C., de Barros Araújo, R., and de Souza Melo, R.J. (2021b). Generalized predictive controller applied in a bidirectional dc-dc converter. In *2021 Brazilian Power Electronics Conference (COBEP)*, 1–6. IEEE.

De Barros Araújo, R., Jeronymo, D.C., and Coelho, A.R. (2016). Hybridization of imc and pid control structures from filtered positional generalized predictive controller. *Proceeding Series of the Brazilian Society of Computational and Applied Mathematics*, 4(1).

Fernandez-Camacho, E. and Bordons-Alba, C. (1995). *Model predictive control in the process industry*. Springer.

Martins, F.C., Gontijo, D.S., and Gonçalves, E.N. (2019). Sıntese de observadores pi baseada em otimizaçao evolutiva multiobjetivo h/h2. *Simpósio Brasileiro de Automação Inteligente-SBAI*.

Santos, T.M.d.O., Ricco, R.A., de Alvarenga Érika Lirena Fonseca Costa, Rivaroli, L., Penoni, Á.C.d.O., and Barroso, M.F.S. (2017). Sintonia ótima do filtro complementar aplicado na junção de sensores inerciais. *Conferência Brasileira de dinâmica, controle e aplicações*.

Seborg, D.E., Edgar, T.F., Mellichamp, D.A., and Doyle III, F.J. (2016). *Process dynamics and control*. John Wiley & Sons.

Silveira, A.S., Rodríguez, J.E., and Coelho, A.A. (2012). Robust design of a 2-dof gmv controller: A direct self-tuning and fuzzy scheduling approach. *ISA transactions*, 51(1), 13–21.

Skogestad, S. and Postlethwaite, I. (2007). *Multivariable feedback control: analysis and design*, volume 2. Citeseer.

Yamaguti, N.N., Dutra, B.G., and Silveira, A.S. (2021). Development of a didactic plant and a human-machine

interface to compare different digital controllers. In *Simpósio Brasileiro de Automação Inteligente-SBAI*, volume 1.